Palaeogeography, Palaeoclimatology, Palaeoecology 301 (2011) 97–107

Contents lists available at ScienceDirect

Palaeogeography, Palaeoclimatology, Palaeoecology

journal homepage: www.elsevier.com/locate/palaeo

The age of the "Grande Coupure" mammal turnover: New constraints from the Eocene–Oligocene record of the Eastern Ebro Basin (NE Spain)

Elisenda Costa *, Miguel Garcés, Alberto Sáez, Lluís Cabrera, Miguel López-Blanco

Grup de Geodinàmica i Anàlisi de Conques (GGAC), Institut de Recerca GEOMODELS, Universitat de Barcelona, Spain
Departament d'Estratigrafia, Paleontologia i Geociències Marines, Facultat de Geologia, Universitat de Barcelona, Martí i Franquès s/n, 08028-Barcelona, Spain

ARTICLE INFO

Article history:
Received 4 February 2010
Received in revised form 11 January 2011
Accepted 12 January 2011
Available online 16 January 2011

Keywords:
Grande coupure
Fossil mammals
Eocene–Oligocene
Magnetostratigraphy
Ebro Basin
SW Europe

ABSTRACT

The Grande Coupure represents a major terrestrial faunal turnover recorded in Eurasia associated with the overall climate shift at the Eocene–Oligocene transition. During this event, a large number of European Eocene endemic mammals became extinct and new Asian immigrants appeared. The absolute age of the Grande Coupure, however, has remained controversial for decades. The Late Eocene–Oligocene continental record of the Eastern Ebro Basin (NE Spain) constitutes a unique opportunity to build a robust magnetostratigraphy-based chronostratigraphy which can contribute with independent age constraints for this important turnover. This study presents new magnetostratigraphic data of a 495-m-thick section (Moià-Santpedor) that ranges from 36.1 Ma to 33.3 Ma. The integration of the new results with previous litho- bio- and magnetostratigraphic records of the Ebro Basin yields accurate ages for the immediately pre- and post-Grand Coupure mammal fossil assemblages found in the study area, bracketing the Grande Coupure to an age embracing the Eocene–Oligocene transition, with a maximum allowable lag of 0.5 Myr with respect to this boundary. The shift to drier conditions that accompanied the global cooling at the Eocene–Oligocene transition probably determined the sedimentary trends in the Eastern Ebro Basin. The occurrence and expansion of an amalgamated-channel sandstone unit is interpreted as the forced response of the fluvial fan system to the transient retraction of the central-basin lake systems. The new results from the Ebro Basin allow us to revisit correlations for the controversial Eocene–Oligocene record of the Hampshire Basin (Isle of Wight, UK), and their implications for the calibration of the Mammal Palaeogene reference levels MP18 to MP21.

1. Introduction

The Grande Coupure was defined by Stehlin (1910) as a major faunal turnover affecting continental vertebrate faunas across Europe occurring close to the Eocene–Oligocene boundary. During this event, a large number of the European Eocene endemic mammals became extinct and new Asian immigrants appeared (Hooker, 1987, 1992; Berggren and Prothero, 1992; Prothero, 1994; Hooker et al., 2004). Only a few families (among them the rodents Theridomyidae and Gliridae) crossed the faunal divide undiminished. Several causes have been proposed as the triggering mechanism for the Grande Coupure; 1) climate deterioration at the Eocene–Oligocene transition (Hartenberger, 1973; Legendre and Hartenberger, 1992); 2) dispersal from outside the main European landmasses (as for instance, through the closing of the Turgai strait which connected continental Europe and Asia during the Eocene; Legendre, 1987; Berggren and Prothero, 1992; Janis, 1993; Prothero, 1994; Akhmetiev and Beniamovski, 2009); and 3) a combination of climate change (cooling) and competition following dispersal into Europe (Hooker et al., 2004). Most recent studies support the idea that climate exercised the prime control on faunal turnover (Joomun et al., 2008), as important crises are recorded in North America (Berggren and Prothero, 1992; Prothero and Swisher, 1992) and Asia (Meng and McKenna, 1998) at apparently the same age. However, despite the consensus among vertebrate palaeontologists on the correlation between the Grande Coupure and the Eocene–Oligocene transition, the precise absolute chronology of this crucial record of the Earth history has remained controversial for decades (Legendre, 1987; Tobien, 1987; Berggren and Prothero, 1992; Hooker, 1992; Legendre and Hartenberger, 1992; Köhler and Moyà-Solà, 1999; and references therein).

In this context, a relevant stratigraphic record is found in the Hampshire Basin of the Isle of Wight (UK), where stratigraphic superposition of marine and continental strata provide direct calibration points with the standard marine chronostratigraphy (Hooker et al., 2004). However, in spite of its ideal stratigraphic setting, the age of the Grande Coupure as recorded in the Solent Group

* Corresponding author. Departament d'Estratigrafia, Paleontologia i Geociències Marines, Facultat de Geologia, Martí i Franquès s/n, 08028-Barcelona, Spain. Tel.: +34 93 4034888; fax: +34 93 4021340.
E-mail addresses: elicosta@ub.edu (E. Costa), mgarces@ub.edu (M. Garcés), a.saez@ub.edu (A. Sáez), lluis.cabrera@ub.edu (L. Cabrera), m.lopezblanco@ub.edu (M. López-Blanco).

0031-0182/$ – see front matter © 2011 Elsevier B.V. All rights reserved.
doi:10.1016/j.palaeo.2011.01.005

has left contrasting results (Hooker et al., 2004, 2007, 2009; Gale et al., 2006, 2007). There, the correspondence between the Grande Coupure and the Eocene–Oligocene transition as proposed by Hooker et al. (2004) was subsequently challenged after an integrated magnetostratigraphy and cyclostratigraphy analysis (Gale et al., 2006), yielding a substantially different age (>2 Ma younger) for the Grande Coupure. Results of Gale et al. (2006) were questioned (Hooker et al., 2007) and, more recently, its magnetostratigraphic correlation re-interpreted (Hooker et al, 2009).

The late Eocene–Oligocene sedimentary record of the central areas of the Eastern Ebro Basin (NE Spain) fully meets the basic requirements of stratigraphic continuity, steady sedimentation, and mammal sites occurrence to build a magnetostratigraphy-based high-resolution continental chronology, as a tool to reliably link marine and continental time scales. In this paper, a new precise chronology across the continuous Eocene–Oligocene continental record in the Ebro Basin is provided. The new chronology further supports the close correlation between the dramatic terrestrial faunal turnover known as the Grande Coupure and the global climate changes that occurred at the Eocene–Oligocene transition.

2. Geological and stratigraphical setting

2.1. The Ebro Basin

The Ebro Basin (Fig. 1 A) represents the latest evolutionary stage of the South Pyrenean foreland system, formed as a result of the collision between the Iberian and the European plates (Muñoz, 1992; Vergés et al., 2002). The basin infill is dominated by continental sediments, interfingered by two widespread marine units of Ilerdian and Lutetian–Bartonian age (Ferrer, 1971; Riba et al., 1983; Puigdefàbregas and Souquet, 1986; Puigdefàbregas et al., 1986; Serra-Kiel et al., 2003; Pujalte et al., 2009). Marine connection of the Ebro Basin was maintained until the Priabonian (Costa et al., 2010), when the tectonic uplift of the western Pyrenees led to the closing of the basin drainage. Since then, uninterrupted late Eocene to middle Miocene continental sedimentation progressively filled the basin and eventually, backfilled onto the thrust-belt margins (Riba et al., 1983; Coney et al., 1996). In the central areas of the basin, this sedimentation was continuous and consisted of lacustrine deposits interfingering red clastic intervals that correspond to the medial-distal parts of fluvial fans draining from the basin margins (Anadón et al., 1989; Arenas et al., 2001; Luzón et al., 2002; Ortí et al., 2007; Sáez et al., 2007; Cuevas et al., 2010).

In the Eastern Ebro Basin, the late Eocene–Oligocene continental succession overlies marine sediments of the Santa Maria Group (Ferrer, 1971; Pallí, 1972; Serra-Kiel et al., 2003) and the halite-dominated Cardona Formation (including its lateral equivalents La Noguera, Artés, and Òdena evaporitic units) (Fig. 1B and C). Integrated calcareous nannofossil and magnetostratigraphic data from the youngest marine units have yielded a Priabonian age (Cascella and Dinarès-Turell, 2009), and the marine-continental transition has been precisely dated at ~36.0 Ma based on magnetostratigraphy (Costa et al., 2010). After the basin closure (Fig. 1B), the lower continental record in the study area corresponds to the Montserrat-Igualada

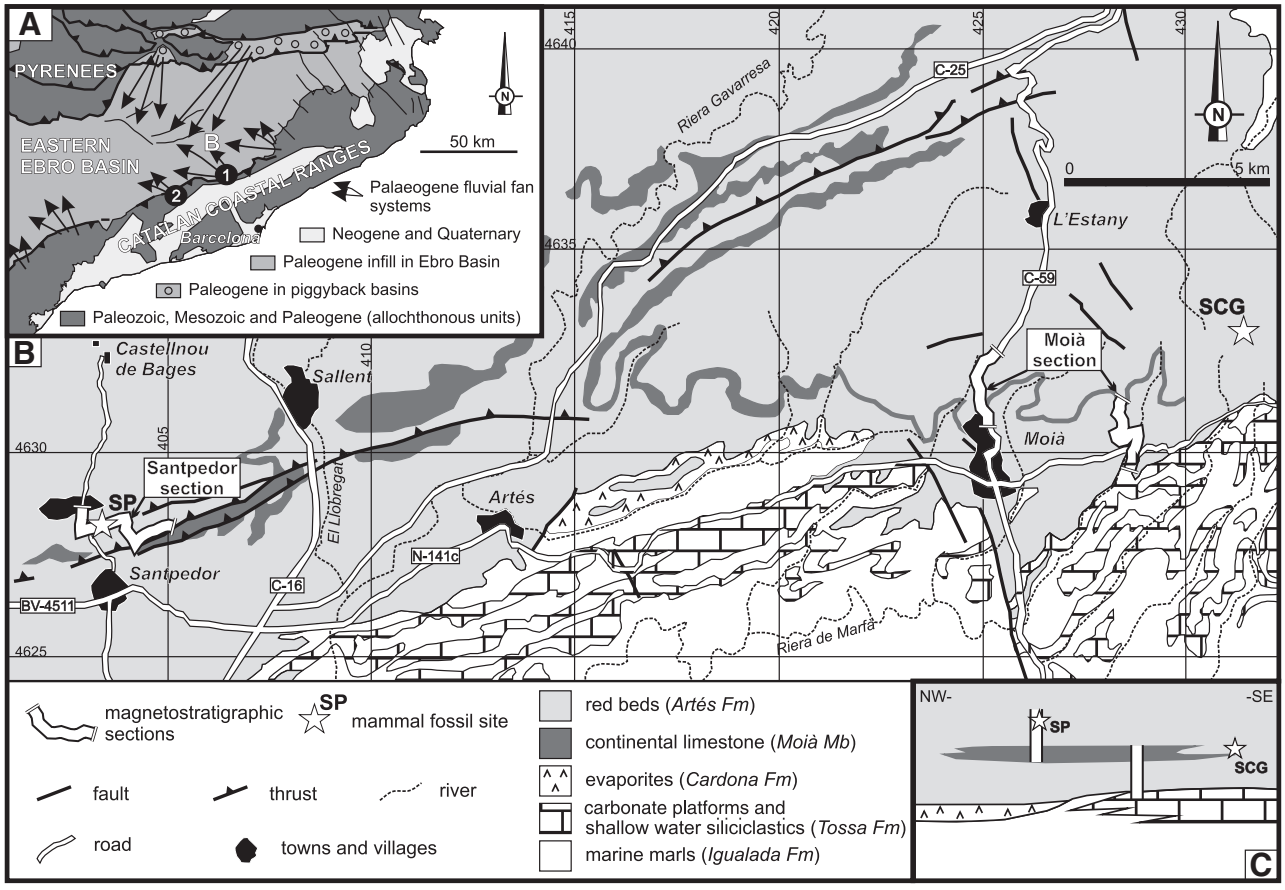

Fig. 1. Geological setting of the Moià-Santpedor composite section. (A) geological map of the Eastern Ebro Basin showing the main fluvial fan systems. 1: Montserrat-Igualada fluvial fan. 2: Montclar-Rocafort fluvial fan. B: location of the detailed geological map of the study area. (B) detailed geological map of the study area and (C) stratigraphy sketch of the SE margin of the Ebro Basin. The Moià and the Santpedor sampled sections are shown and the Sant Cugat de Gavadons (SCG) and Santpedor (SP) fossil assemblages are indicated with a white star symbol. A complete faunistic list for these localities is available at Agustí et al. (1987), Anadón et al. (1987, 1992), Sáez (1987), Arbiol and Sáez (1988). The lithostratigraphic correlation between the Moià and the Santpedor sections was established using the distinctive limestone beds of the Moià Limestone Member (Based in Sáez, 1987; Sáez et al., 2007). Map coordinates are in UTM projection, ED50 / zone 31.

fluvial fan (Sáez, 1987; Fig. 1A for location) that comprises the alluvial sediments of the Artés Formation (Ferrer, 1971) and the lacustrine limestones of the Moià Member of the Castelltallat Formation (Sáez, 1987; Sáez et al., 2007). Late Eocene (Sant Cugat de Gavadons) to Early Oligocene (Santpedor) vertebrate fossil assemblages have been reported in the basal sediments of the Artés Formation (Agustí et al., 1987; Anadón et al., 1987, 1992; Sáez, 1987; Arbiol and Sáez, 1988). Younger units south westwards have provided a complete Oligocene magnetostratigraphic record which contributed to the age calibration of the Western Europe MP mammal biochronology (Barberà, 1999; Barberà et al., 2001).

2.2. The Moià-Santpedor composite section

The medial-distal fluvial fan deposits of the Artés Formation consist of about 1000 m of red mudstones with some intervals of fluvial channel sandstones. One of these sandstone intervals is the Santpedor sandstone unit (Sáez, 1987). The Santpedor sandstone unit is composed of amalgamated incised channelled sandstone to gravelly sandstone beds, sourced from the Catalan Coastal Ranges (Sáez, 1987). This competent unique 20-m-thick coarse-grained unit is a continuous and extensive (traceable over most of the eastern margin of the Ebro Basin) key bed despite its variable thickness due to its erosive fluvial origin. Also intercalated into the Artés Formation, the 100-m-thick Moià Member consists of decimetre to metre-thick beds of lacustrine micritic limestone gently dipping <10° to the NW. In this sedimentary record, two sections (Moià and Santpedor) were sampled for magnetostratigraphy. A solid correlation between sections was established using the limestone key beds present in the Moià Member, yielding a 495-m-thick composite succession (see Fig. 1B and C).

Mammal biochronological constraints within the studied sections include the Late Eocene site of Sant Cugat de Gavadons and the Early Oligocene site of Santpedor (Fig. 1B and C). The Sant Cugat de Gavadons fossil site is located 4 km NE from Moià and can be correlated with the studied section according to Anadón et al. (1987). Its faunal assemblage is included in the *Theridomys golpeae* Biozone of the local biozonation of the Ebro Basin, and correlated to the pre-Grande Coupure MP19–20 European reference level (Agustí et al., 1987; Anadón et al., 1987, 1992; Sáez, 1987; Arbiol and Sáez, 1988). More recently, Hooker et al. (2009) suggested an alternative correlation of the Sant Cugat de Gavadons, as well as the Rocafort de Queralt (Anadón et al., 1987), with MP18, arguing that none of the taxa in these sites is diagnostic of the MP19–20, and most of them range at least from the MP18 to the MP20.

Of particular relevance for this study is the Early Oligocene (MP21) fauna of Santpedor. According to Agustí et al. (1987), Anadón et al. (1987, 1992), Sáez (1987), and Arbiol and Sáez (1988) the Santpedor fossil site contains *Theridomys* aff. *aquatilis*, *Gliravus* aff. *priscus*, *Pseudoltinomys gaillardi*, *Eucricetodon atavus*, *Plagiolophus annectens*, *Palaeotherium medium* and an undetermined Anoploteridae. This fossil site is directly located in the upper part of the Santpedor section only a few meters above the Santpedor sandstone unit (Figs. 1B and C).

3. Palaeomagnetic analysis

3.1. Sampling and methods

A total of 191 palaeomagnetic sites were sampled at a mean resolution of about 2.6 m, which is sufficient to allow a complete identification of the Upper Eocene–Lower Oligocene geomagnetic polarity reversals considering mean accumulation rates of about 10–15 cm/kyr reported in neighbouring areas of the Ebro Basin (Vergés et al., 1998; Barberà et al., 2001). Fine-grained sediments are abundant through the section, and sampling was focused on both red mudstones and white micritic limestones. At least, 2 oriented cores per site were obtained with an electrical portable drill and oriented in situ using a magnetic compass with inclinometer.

The palaeomagnetic analyses consisted in stepwise thermal demagnetization of the natural remanent magnetization (NRM) of at least one sample per site. In order to characterize the magnetic carriers, additional alternating field (AF) demagnetization of the NRM and progressive IRM acquisition and subsequent three-axial IRM demagnetization were conducted in a selected set of samples. Measurements of the magnetic remanence were performed using 2G superconducting rock magnetometers at the Palaeomagnetic Laboratories of the universities of Barcelona (Serveis Cientificotècnics UB-CSIC) and Utrecht. Stepwise thermal demagnetization was conducted in a Schönstedt TSD-1 thermal demagnetizer and a laboratory-built furnace (Utrecht) at intervals ranging between 10 °C and 50 °C and up to a maximum temperature of 680 °C. Magnetic susceptibility was also measured after each demagnetization step using a KLY-2 magnetic susceptibility bridge (Geofizika Brno). AF demagnetization, performed in an ASC D-Tech2000 alternating field demagnetizer, included a maximum of 12 steps with intervals of 5 mT, 10 mT, 20 mT and 50 mT up to 200 mT. Progressive IRM acquisition was carried out by means of an ASC IM10–30 pulse magnetizer up to a maximum pulse field of 1200 mT. Following Lowrie (1990), three fields of 1200 mT, 300 mT and 60 mT were respectively applied in the z, y and x sample axis for the subsequent thermal demagnetization of the samples.

3.2. Magnetic properties

The Zijderveld plots and the IRM experiments (Fig. 2) show that the behaviour of the NRM is related to lithology. In the white limestone samples (Fig. 2A–D) the NRM consist of two magnetic components: a viscous component and a high temperature stable component. The viscous component is unblocked at temperatures below 240 °C to 310 °C and parallels the present day field. The stable component, which yields maximum unblocking temperatures near 400 °C, shows both normal and reversed polarities and has been considered the characteristic remanent magnetization (ChRM). These two components are also observed in the AF demagnetization (Fig. 2B), being the samples completely demagnetized at peak fields of 60 mT. The saturation of the IRM of the white limestone samples is not achieved at the maximum fields of 1200 mT, but 80% of the remanence is achieved at relative low fields ~100 mT (Fig. 2C) and the soft component fraction (60 mT) demagnetizes completely below 480 °C (Fig. 2D). The NRM unblocking temperatures and coercivity spectra, together with the IRM acquisition and demagnetization data suggest the presence of magnetite as the principal magnetic carrier in the white limestone samples.

In the red bed samples (Fig. 2 E–L) a viscous component of the NRM is removed after heating to 250–300 °C. Further heating reveals a ChRM component with maximum unblocking temperatures ranging from 640 °C to 680 °C (Fig. 2 E and I). In addition, red bed samples having a normal polarity ChRM component, often reveal the presence of an intermediate component of reversed polarity (Figs. 2 I and 3 B). This intermediate component shows maximum unblocking temperatures ranging from 500 °C to 640 °C. The AF demagnetization of the red bed samples (Fig. 2 F and J) is only capable of removing a small fraction of the NRM at the maximum field of 200 mT, this corresponding to the soft viscous component. The IRM acquisition experiments (Fig. 2 G and K) yield unsaturated curves typical of high-coercivity minerals. Thermal demagnetization of both intermediate and hard-fraction coercivity fractions (300 mT and 1200 mT respectively) shows a maximum unblocking temperature of ~640 °C. It is concluded that, independently of the number of palaeomagnetic components contributing to the NRM, red bed samples depict a similar behaviour during the IRM experiments (Fig. 2 E–L), suggesting the same magnetic fraction composition. According to both the NRM and IRM unblocking

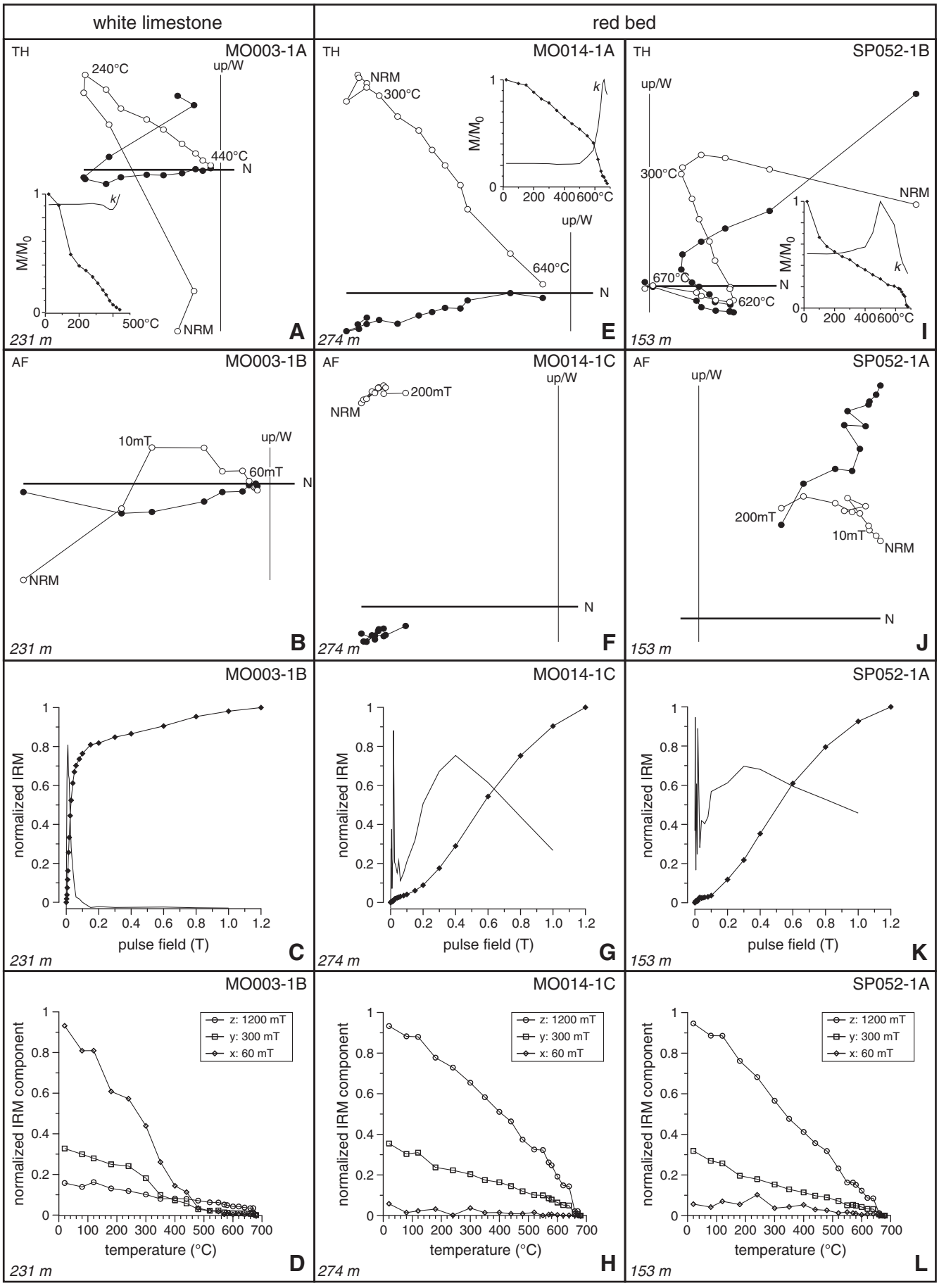
white limestone
red bed
TH
MO003-1A
240°C
up/W
440°C
N
NRM
k
M/M0
500°C
231 m
A
TH
MO014-1A
NRM
300°C
640°C
up/W
N
274 m
E
TH
SP052-1B
up/W
300°C
NRM
670°C
620°C
N
153 m
I
AF
MO003-1B
10mT
up/W
60mT
N
NRM
231 m
B
AF
MO014-1C
up/W
200mT
NRM
N
274 m
F
AF
SP052-1A
up/W
200mT
10mT
NRM
N
153 m
J
MO003-1B
normalized IRM
pulse field (T)
231 m
C
MO014-1C
normalized IRM
pulse field (T)
274 m
G
SP052-1A
normalized IRM
pulse field (T)
153 m
K
MO003-1B
normalized IRM component
z: 1200 mT
y: 300 mT
x: 60 mT
temperature (°C)
231 m
D
MO014-1C
normalized IRM component
z: 1200 mT
y: 300 mT
x: 60 mT
temperature (°C)
274 m
H
SP052-1A
normalized IRM component
z: 1200 mT
y: 300 mT
x: 60 mT
temperature (°C)
153 m
L

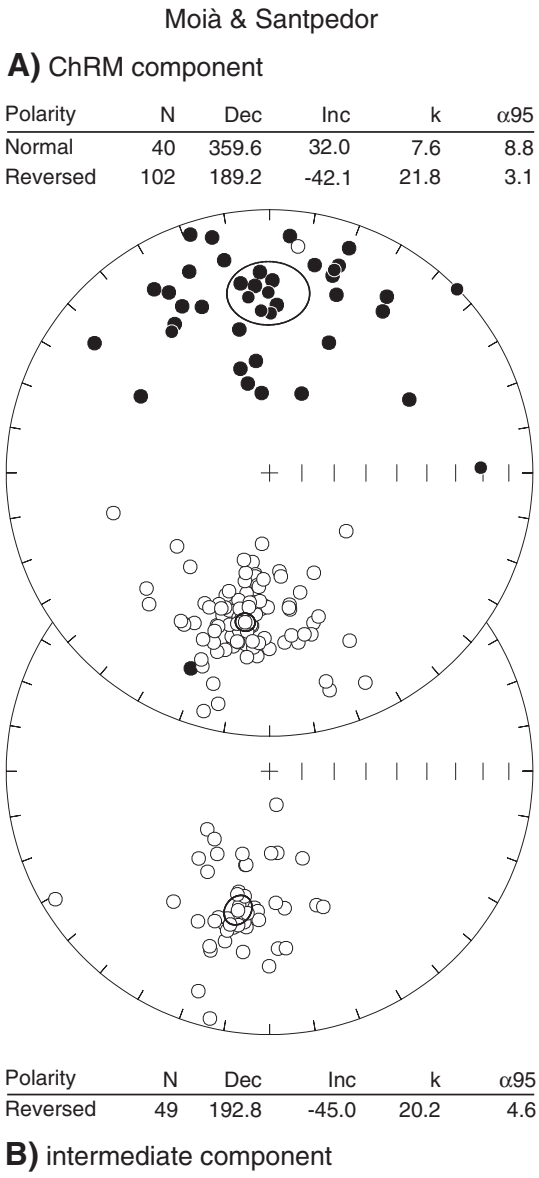

Fig. 3. Stereonet projection of the ChRM (A) and the intermediate component of the red beds (B) on the Moià-Santpedor composite section with calculated Fisherian means and statistics.

temperatures and the coercivity spectra, the magnetic fraction is dominated by haematite. Grain-size dependence of rock-magnetic properties in natural haematite as well as correspondence with remanence acquisition mechanisms in red beds has been reported in Dekkers and Linssen (1989). Therefore, the presence of two distinct magnetic components carried by haematite could be related to a bimodal grain-size distribution. Coarse-grained detrital haematite grains could be the carrier of the high-temperature ChRM, whereas fine-grained haematite cement would be responsible for the intermediate component acquired in a later burial stage. The nature and origin of this intermediate component will be discussed further (see Section 5.1.).

3.3. Magnetic stratigraphy of Moià-Santpedor

Palaeomagnetic components were calculated by means of least squares analysis (Kirschvink, 1980). The normal and reversed ChRM directions yield antipodal Fisherian means (Fig. 3 A) which conform to the palaeomagnetic references for the Late Eocene to Early Oligocene (Barberà, 1999; Costa et al., 2010). The reversed secondary component yielded a mean value which is also concordant with the ChRM mean direction (Fig. 3B).

ChRM directions were used to compute the latitude of the virtual geomagnetic pole (VGP) in order to obtain a local magnetic stratigraphy of the Moià-Santpedor composite section (see Supporting Table 1). Magnetozones were defined by at least two adjacent palaeomagnetic sites with the same polarity. Single-site reversals were denoted as half bar magnetozone in the local magnetostratigraphy, but were not used for magnetostratigraphic correlation purposes. Because of the existence of a widespread secondary magnetization of reversed polarity, we were cautious in the interpretation of stratigraphic intervals with alternating normal and reversed polarities. After the exclusion of these unreliable short events, a total of 7 magnetozones have been recognised along the 495-m-thick Moià-Santpedor local magnetostratigraphy (Fig. 4).

4. Correlation with the geomagnetic polarity time scale

A unique correlation of the local magnetostratigraphy of Moià-Santpedor with the Geomagnetic Polarity Time Scale (GPTS) 2004 (Gradstein et al., 2004) can be put forward on the basis of the available litho- and chronostratigaphic constraints (Fig. 5). First, the age of the marine-continental transition in the Ebro Basin, recorded at the bottom of the studied sections, has been recently correlated with chron C16n, at about 36 Ma, Priabonian (Costa et al., 2010). Second, a lithostratigraphic correlation between the Moià-Santpedor and the Maians-Rubió sections (Fig. 5 A and B) is feasible on the basis of the cartographic expression of the Santpedor sandstone unit.

The best fit of our composite magnetostratigraphy with the GPTS (Gradstein et al., 2004) is established by correlating with the range of chrons C16n.2n to chron C13n of the Late Eocene–Early Oligocene (Fig. 5). The short reversed magnetozone R1 correlates to C16n.2r, a subchron which was not confidently identified in the Maians-Rubió local magnetostratigraphy of Costa et al. (2010). Average sedimentation rates of about 20 cm/kyr are calculated for the Moià-Santpedor composite section, in close agreement with the observed trends in late Eocene–early Oligocene sections of the Eastern Ebro Basin (Barberà et al., 2001; Costa et al., 2010; Fig. 5 B, D and E).

5. Discussion

5.1. The sedimentary record of the Eocene–Oligocene transition in the Ebro Basin

According to the new magnetostratigraphic data and the derived average sedimentation of the Moià-Santpedor composite section (Fig. 5 E), the Eocene–Oligocene boundary can be placed by interpolation at ~80 m below the Santpedor fossil locality (see Figs. 4 and 5). 30 meters above the Eocene–Oligocene boundary and coinciding with the base of the chron C13n, the Santpedor sandstone unit occurs. This unit, which is interbedded within the red mudstone-dominated distal fluvial fan succession marks a progradation of the overall fluvial fan systems, as it is also recognised southwestwards in

Fig. 2. Representative palaeomagnetic results of the different studied rock types from the Moià and Santpedor sections. The stratigraphic position is shown in meters. (A), (E) and (I) shows the Zijderveld diagrams of the stepwise thermal demagnetization process. The NRM decay plots (squared curve) are obtained after the normalization of the vector subtraction module. The magnetic susceptibility (*K*) is also plotted. (B) AF demagnetization diagram of a white limestone sample kind. (F) and (J) show also AF demagnetization for the red beds samples, note how only the viscous component is demagnetized in these samples. All the thermal and AF demagnetization projections are in tectonic corrected coordinates. Progressive acquisition IRM curves for a white limestone sample (C) and for the one and two components of the red bed samples (G and K). (D), (H) and (L) three-axial IRM demagnetization curves following Lowrie (1990).

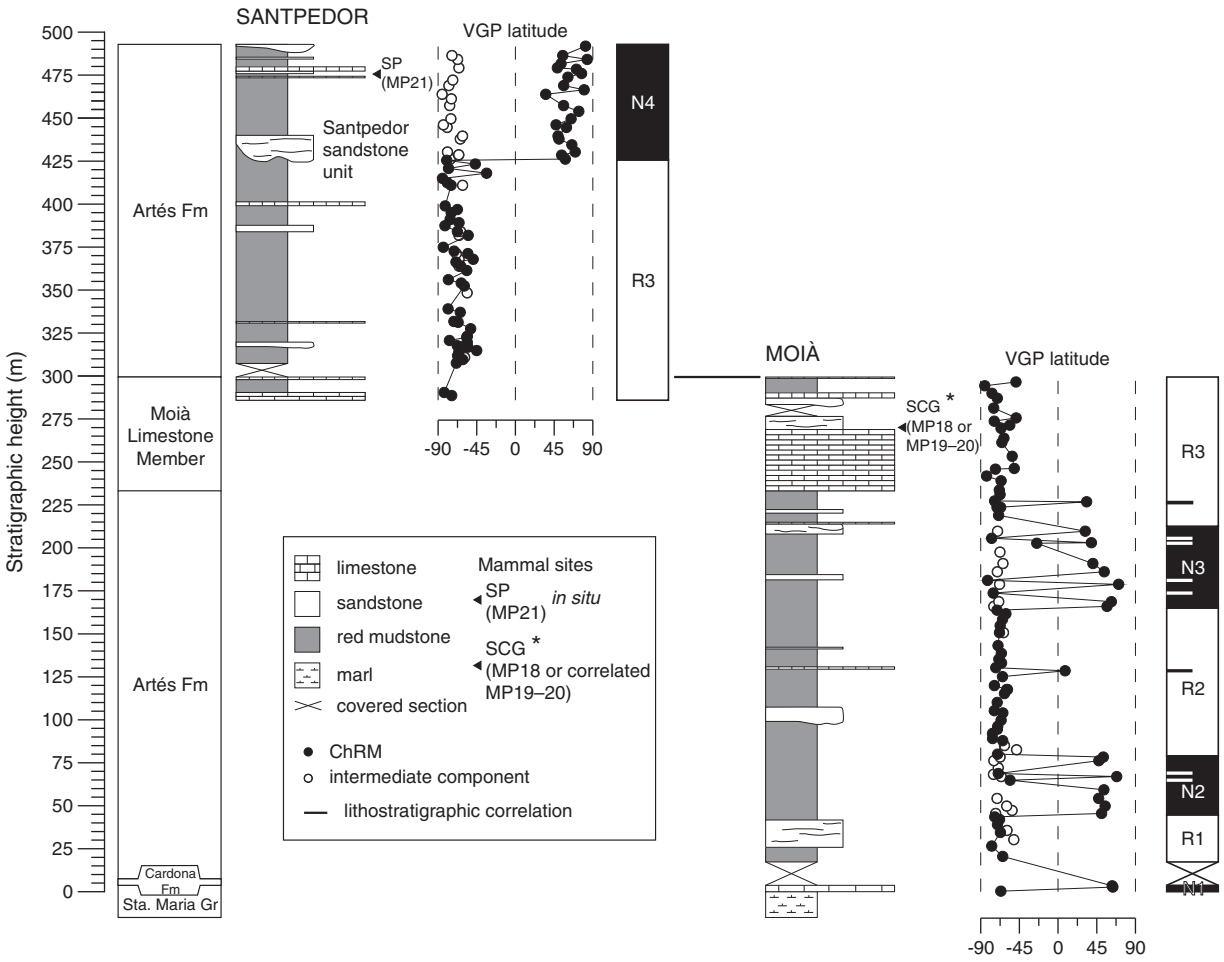

Fig. 4. Local litho- and magnetostratigraphic sections of Moià and Santpedor. The correlation between sections, which was established using the distinctive limestone beds of the Moià Limestone Member (see Figs. 1B and C), is also shown. The location of fossil mammal sites and their attribution to the MP reference levels are indicated. SCG, Sant Cugat de Gavadons. SP, Santpedor. Asterisk (*) indicates fossil mammal site correlated to the magnetostratigraphic section. Circles show the VGP latitude. Solid symbol is used for the ChRM component while open symbol indicates the presence of an intermediate component of exclusively reversed polarity. Stable magnetozones were defined by at least 2 adjacent palaeomagnetic sites showing the same polarity. Half bar zones denote one site reversals.

the Montclar-Rocafort fluvial fan succession as a sharp transition from lacustrine to alluvial deposits (Fig. 5; Fig. 1 A for Montclar-Rocafort fluvial fan location).

The age correspondence with the base of the chron C13n, and thus to the Oi-1 event (Katz et al., 2008) advocates a climate control on the expansion of the Santpedor sandstone unit (Figs. 5 and 7). Sedimentological data suggest that climate forcing was transmitted by a drop in the base level of the basin, similar to those described in the fluvial fan deposits of the Pyrenean margin (Sáez et al., 2007). The retraction of the central-basin lake systems and the basinwards expansion and incision of the fringing fluvial fans is interpreted as a response to the aridification process that accompanied the Late Eocene–Oligocene global cooling. Evidences of this palaeoenvironmental aridification are found in the Late Eocene Ebro Basin palaeofloral record (Cavagnetto and Anadón, 1996; Barberà et al., 2001) as well as in vast regions of Eurasia (Collinson and Hooker, 2003; Dupont-Nivet et al., 2007; Akhmetiev and Beniamovski, 2009).

Environmental changes occurring during the Eocene–Oligocene transition probably affected early burial diagenetic conditions in the alluvial sediments of the Ebro Basin. A consequence of shifting burial conditions could be the pervasive reversed-polarity secondary magnetization found in this study (Fig. 3 B and open symbol in Fig. 4; see Section 3.2.), as well as in the late Eocene sediments of the Maians-Rubió section (Costa et al., 2010). The fact that no equivalent signatures are reported in the younger Oligocene sediments in the Ebro Basin lead us to suggest that this single-polarity secondary magnetization is linked to a unique event. It is hypothesized that deepening of the phreatic levels could have enhanced the acquisition of a late magnetization via renewed oxidation of buried sediments, and precipitation of haematite cement in sediment porosity. Examples of a secondary magnetization linked with the drop of phreatic levels are found in the younger Messinian sediments of the Fortuna Basin (Garcés et al., 2001).

5.2. The age of the Grande Coupure

The magnetostratigraphy-based chronology of the Moià-Santpedor section allows the establishment of a reliable chronostratigraphy of the late Eocene to the early Oligocene continental record of the Eastern Ebro Basin. These results provide an age of 33.4 Ma (within the chron C13n) for the Santpedor fossil site, supporting an earliest Oligocene age, as envisaged from its biochronological ascription (Agustí et al., 1987; Anadón et al., 1987, 1992; Sáez, 1987; Arbiol and Sáez, 1988). Likewise, the age of the pre-Grande Coupure site of Sant Cugat de Gavadons can be estimated to about 34.5 Ma. These results bracket the Grande Coupure to an age interval embracing the Eocene–Oligocene boundary, dated at 33.9 Ma (Gradstein et al., 2004). Further, the Santpedor fossil assemblage is of special interest because of the rare coexistence of pre- and post-Grande Coupure fauna (Agustí et al., 1987; Hooker et al., 2009). Thus, if Santpedor is to be considered

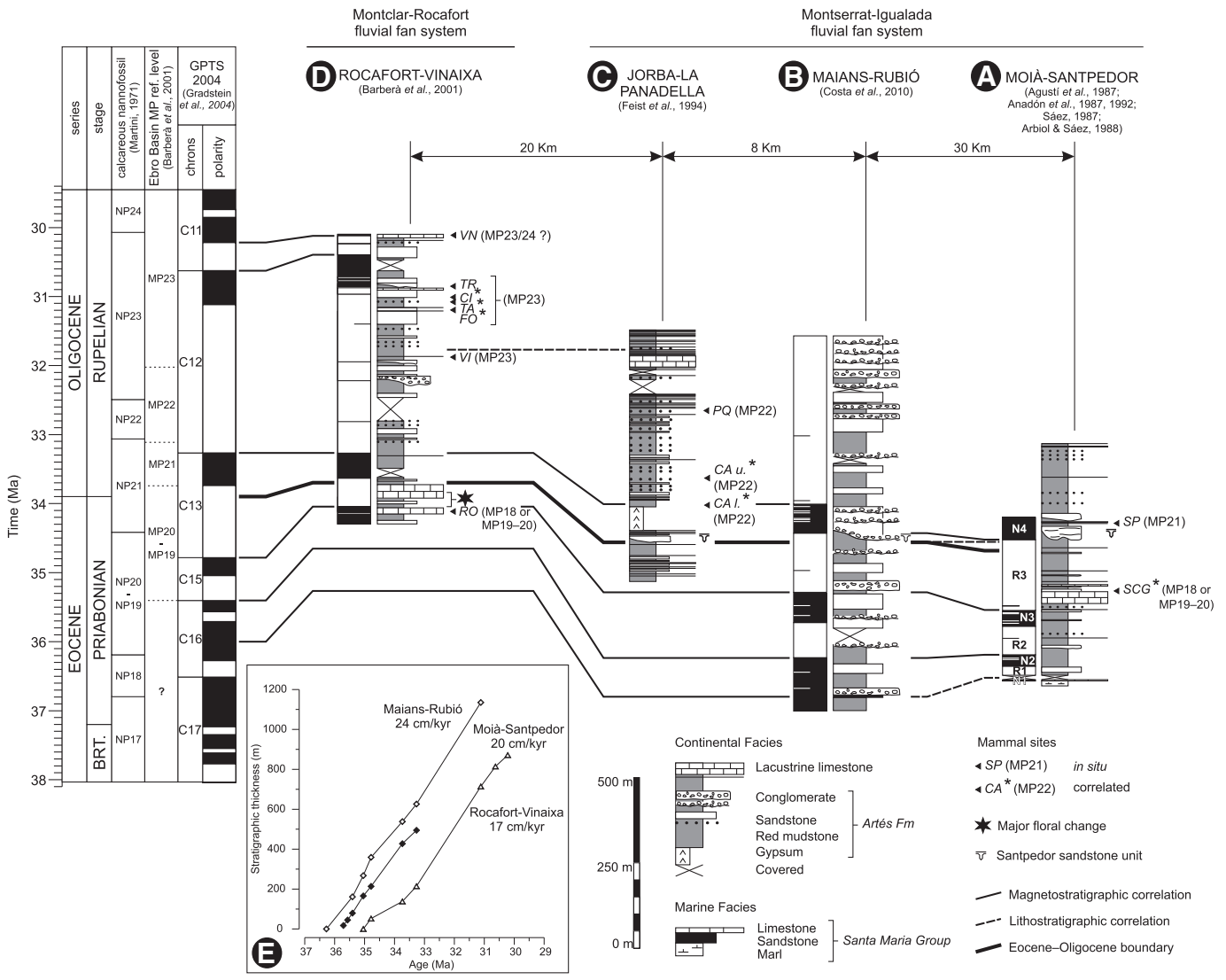

Fig. 5. Correlation of the local magnetostratigraphy of the Moià-Santpedor composite section (A) to the GPTS (Gradstein et al.;, 2004) with indication of the vertebrate localities and their corresponding MP reference levels (Agustí et al., 1987; Anadón et al., 1987, 1992; Sáez, 1987; Arbiol and Sáez, 1988; Barberà et al., 2001). SCG, Sant Cugat de Gavadons. RO, Rocafort de Queralt. SP, Santpedor. CA l., Lower Calaf. CA u., Upper Calaf. PQ, Porquerisses. VI, Vimbodí. FO, Forés. TA, Tàrrega. CI, Ciutadilla. TR, Tarrés. VN, Vinaixa. Asterisk (*) indicates fossil mammal site correlated to the sections. The Rocafort-Vinaixa log (D) is a composite section from the Rocafort, Sarral, Solivella, Tarrés and Vinaixa magnetostratigraphic sections of Barberà et al. (2001). The Jorba-La Panadella lithostratigraphic section (C) (Feist et al., 1994) correlates the Maians-Rubió composite section (B) of Costa et al. (2010) with the Rocafort-Vinaixa section of Barberà et al. (2001) The regional significant Santpedor sandstone unit has been used to correlate the Moià-Santpedor composite section with the magnetostratigraphic composite sections of Maians-Rubió (Costa et al., 2010) and Rocafort-Vinaixa (Barberà et al., 2001). (E) accumulation curves and the mean sedimentation rates derived from the proposed correlation of the Moià-Santpedor local magnetostratigraphy are also compared to the values for the Maians-Rubió (Costa et al., 2010) and Rocafort-Vinaixa (Barberà et al., 2001).

among the oldest post-Grande Coupure records, a (maximum) lag of 0.5 Myr relative to the Eocene–Oligocene boundary is determined.

5.3. Correlation between the Ebro and the Hampshire basins

The age of the Grande Coupure in the Hampshire Basin (Isle of Wight, UK) has become controversial since Gale et al. (2006) provided the Solent Group succession with a first magnetostratigraphy (Gale et al., 2006, 2007; Hooker et al., 2007, 2009). For the sake of clarity, we summarize in Fig. 6 all the alternative magnetostratigraphic correlations of the Solent Group succession with the GPTS (Gradstein et al., 2004). Gale et al. (2006) substantiated their correlation according solely to the presence of diagnostic nannofossils *Discoaster saipanensis* and *Ismolithus recurvus* of the Zone NP19–20 in the Brockenhurst Bed, located at the base of the sampled section (Fig. 6 A). Following this constraint, they correlated the lower thick normal magnetozone to the chron C15n and found a best match by correlating their Bembridge Normal Polarity Zone (BNPZ) to the chron C13n. This correlation yielded an age for the Grande Coupure (MP20–MP21 boundary) about 2 Myr younger than the Eocene–Oligocene boundary, being in apparent contradiction with previous chronostratigraphic interpretations of the Solent Group succession (Hooker, 1992; Hooker et al., 2004).

Alternative correlations for the Solent Group succession were put forward in order to reconcile magnetostratigraphy and mammal biochronology (Hooker et al., 2007, 2009) (Fig. 6 B and C). Hooker et al. (2009) favoured a correlation of the basal normal magnetozone in the Solent Group succession with chron C16n since this option was also in accordance with the range of the Zone NP19–20 (Gradstein et al., 2004). Hooker et al. (2009) also proposed the correlation of the BNPZ to C13r.1n, a short subchron not present in the GPTS 2004 (Gradstein et al., 2004), but recorded at Site 1090 of the South Atlantic Ocean (Channell et al., 2003). The existence of subchron C13r.1n, however, is controversial since it has not been recorded in other high-

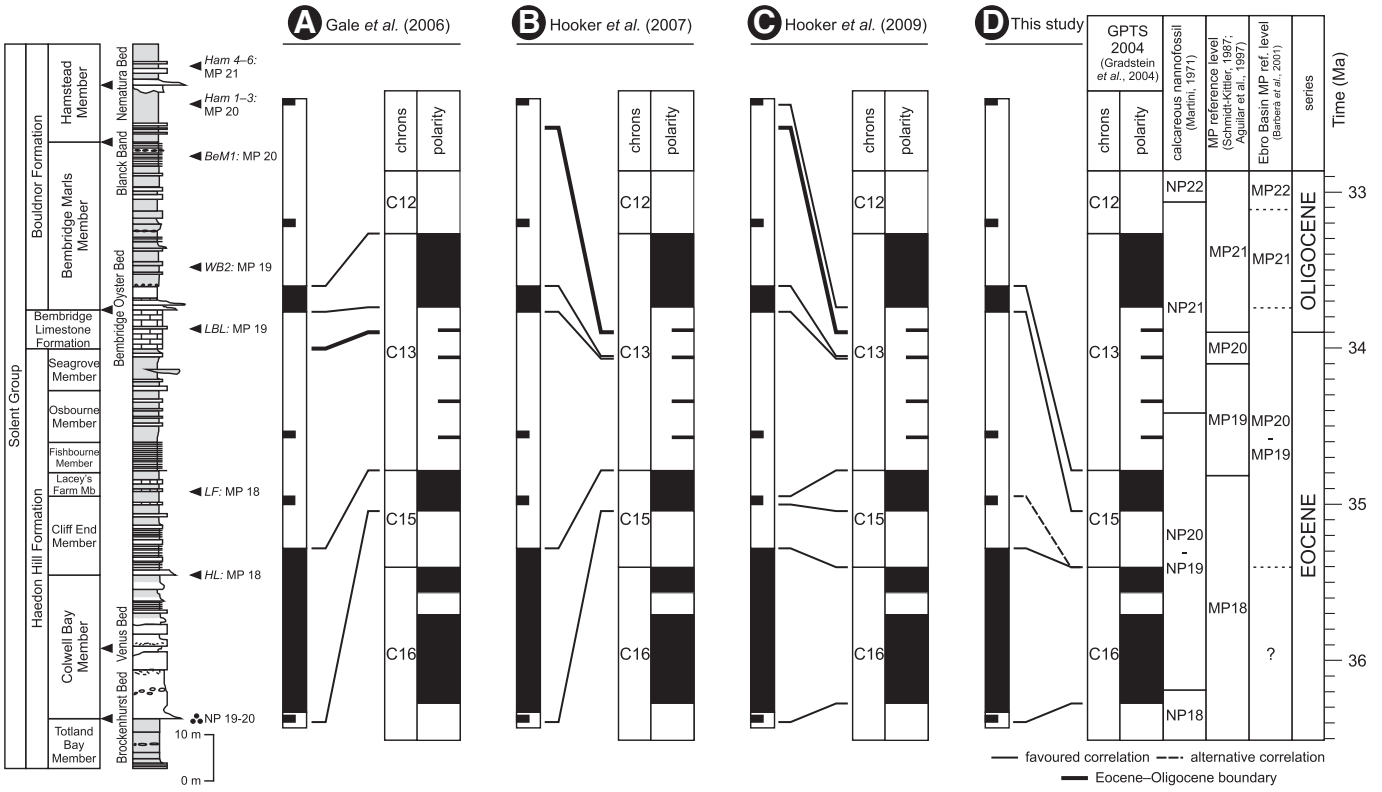

Fig. 6. Successive proposed correlations for the magnetostratigrapic record of the Solent group in the Hampshire Basin (Isle of Wight, UK). Litho- and magnetostratigraphic information come from Gale et al. (2006). Biochronological information has been compiled from Hooker (1992, 2010); Hooker et al. (2004, 2007, 2009), and Gale et al. (2006). HL, Hartherwood Lignite Bed. LF, Lacey's Farm Member. LBL, Limestone of the Bembridge Limestone Formation. WB2, Whitecliff Bay 2. BeM1, Bembridge Marls 1. Ham 1–3, Hampstead Member 1, 2 and 3. Ham 4–6, Hampstead Member 4, 5 and 6. The location of the Eocene–Oligocene boundary according to different options is marked with a thick black line. Subchrons in chron C13r come from Cande and Kent (1995).

resolution records elsewhere (Lowrie and Lanci, 1994; Lanci et al., 1996; Parés and Lanci, 2004). The correlation proposed by Hooker et al. (2009) yields a considerable mismatch with the pattern of chrons of the GPTS since a short, single-site magnetozone is correlated with chron C15n while the thicker BNPZ is correlated with C13r.1n, a short event of unknown nature (cryptochron or subchron), duration and age (Fig. 6 C).

Further arguments to constrain the correlation of the BNPZ with the GPTS rely on the biomagnetostratigraphic record of the Ebro Basin (Barberà et al, 2001) and the biochronological interpretation of the Sant Cugat de Gavadons mammal site. As discussed above (Section 2.2.), Hooker et al. (2009) assigned to this locality a MP18 age, while the magnetostratigraphy of the Moià-Santpedor composite section dictates a correlation of this site with chron C13r. Since the BNPZ in the Solent Group succession is found associated to fossil sites of MP19 age, Hooker et al. (2009) derived that BNPZ must correlate to a normal subchron within C13r (Fig. 6 C).

It must be noted, however, that consensus on the biochronological significance of Sant Cugat de Gavadons is not yet reached. The endemism affecting fossil assemblages of the Ebro Basins (Badiola et al., 2009) has possibly hampered the establishment of a robust biochronology linking both regions. Therefore, it is worth considering the alternate scenario where Sant Cugat de Gavadons is assigned to MP19–20, following Agustí et al. (1987), Anadón et al. (1987; 1992) and Badiola et al. (2009). Under this assumption, a correlation of the BNPZ with chron C15n is derived (Fig. 6 D), leaving uninterpreted (unreliable) all single-site normal magnetozones in the Solent Group succession (Fig. 6 D). Such alternative was already analysed by Gale et al. (2007) in their reply to Hooker et al. (2007), but rejected arguing that the magnetostratigraphic data from the Ebro Basin (Barberà et al., 2001) were not as reliable to be taken into account (Gale et al., 2007).

5.4. Implications for the European land mammal chronology

This paper contributes to further support to the magnetostratigraphy-based chronological framework of the Eocene–Oligocene sedimentary record of the Ebro Basin (Barberà et al., 2001). Its significance for the calibration of the European Land Mammal chronology should be discussed in the light of the endemism of Iberian faunas with respect to the central European MP reference levels (Badiola et al., 2009). Regarding the Late Eocene, the uncertain biochronological assignment of the fossil assemblage of Sant Cugat de Gavadons has led to two alternative correlations of the Solent Group succession in the Hampshire Basin (Fig. 7, see discussion above). Option A follows Hooker et al. (2009), and results in a calibration of the MP19, MP20 and MP21 units within a very short-ranged time span. In Option B the alternative correlation of the Solent Group succession with the GPTS 2004 (Gradstein et al., 2004) as discussed in Section 5.3. is considered. Option B assigns a longer duration for the MP zones with the MP18 and MP19 zones pinned down to an age older than the presently accepted (Schmidt-Kittler, 1987; Aguilar et al., 1997). Earlier calibrations constrained the age of the MP20 reference level to a short period of 200 kyr at precisely the latest Eocene (Schmidt-Kittler, 1987; Aguilar et al., 1997). Based on limits derived from Option B, MP20 is correlated within chron C13r, but its exact age and duration is not so tightly constrained (Fig. 7).

Finally, a minimum age of 33.4 Ma is determined for the MP21 reference level, based on the calibration of the locality of Santpedor in the Ebro Basin (Fig. 7). The MP21 locality high in the Hampshire Basin succession (Ham 4–6) does not provide further constraints since it lacks magnetostratigraphy (Fig. 6). This lead to the conclusion that, considering the magnetostratigraphy-based ages of the MP20 and MP21 reference levels, the Grande Coupure lags the Eocene–

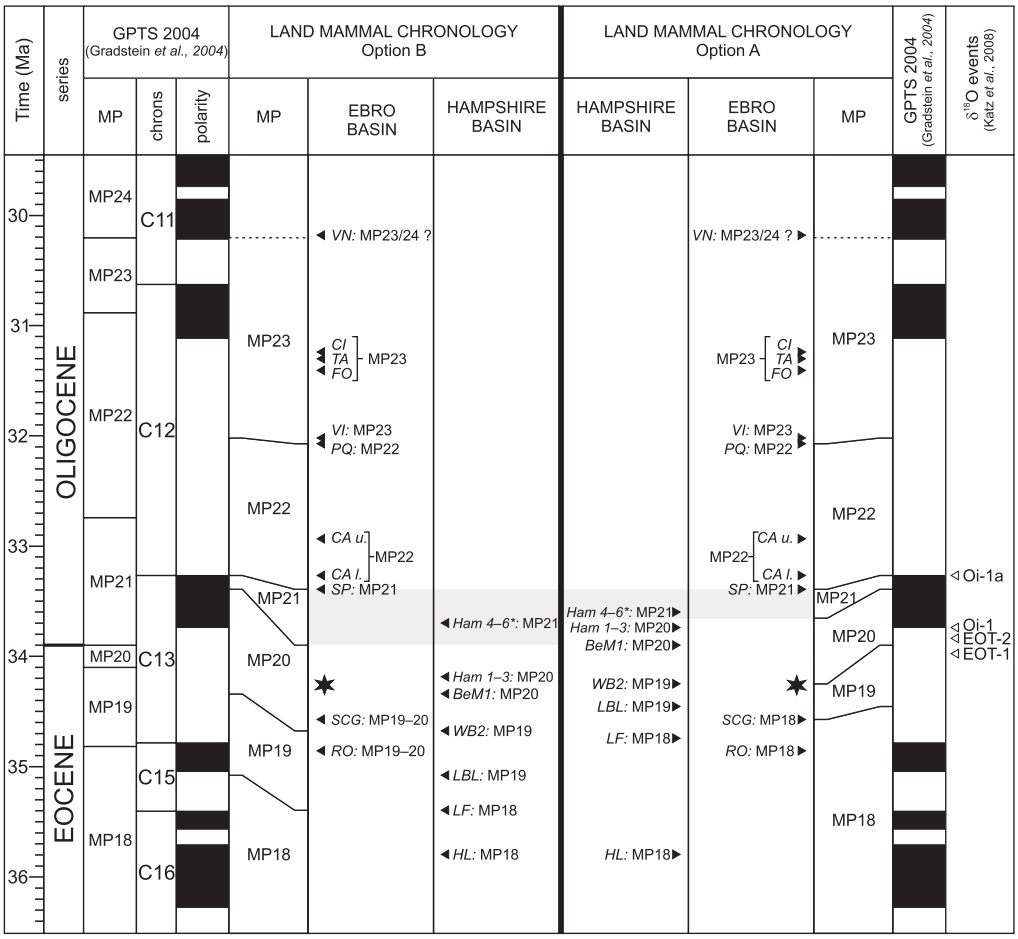

Fig. 7. Calibration of the MP reference levels to the GPTS (Gradstein et al., 2004) across the Eocene–Oligocene boundary. Biostratigraphic data of the Eastern Ebro Basin comes from Agustí et al. (1987), Anadón et al. (1987, 1992), Sáez (1987), Arbiol and Sáez (1988), Barberà et al. (2001), and this study. SCG, Sant Cugat de Gavadons. RO, Rocafort de Queralt. SP, Santpedor. CA l., Lower Calaf. CA u., Upper Calaf. PQ, Porquerisses. VI, Vimbodí. FO, Forés. TA, Tàrrega. CI, Ciutadilla. TR, Tarrés. VN, Vinaixa. The star symbol indicates major floral change in the Ebro Basin (Cavagnetto and Anadón, 1996; Barberà et al., 2001). Biostratigraphic data of the Hampshire Basin comes from Hooker (1992, 2010) and Hooker et al. (2004, 2007, 2009). HL, Hartherwood Lignite Bed. LF, Lacey's Farm Member. LBL, Limestone of the Bembridge Limestone Formation. WB2, Whitecliff Bay 2. BeM1, Bembridge Marls 1. Ham 1–3, Hampstead Member 1, 2 and 3. Ham 4–6, Hampstead Member 4, 5 and 6. Asterisk (*) in Ham 4–6 indicates no direct magnetostratigraphic data available (see Fig. 6). Option A: assumes an MP18 age for the SCG and RO fossil localities in the Eastern Ebro Basin (Hooker et al., 2009) and the correlation of the MP reference levels in the Hampshire Basin (Isle of Wright, UK) follows Hooker et al. (2009) correlation to the GPTS. Option B: assumes an MP19–20 age for the SCG and RO fossil localities in the Eastern Ebro Basin (Agustí et al., 1987; Anadón et al., 1987, 1992) and the calibration of the fossil sites in the Hampshire Basin (Isle of Wright, UK) is derived from the alternative correlation to the GPTS proposed in Fig. 6D (see text for discussion). Grey-shaded area indicates the possible range of the Grande Coupure for both options.

Oligocene boundary by a maximum of 0.5 Myr as shown with the grey-shaded areas in Fig. 7.

6. Conclusions

New magnetostratigraphic data of the 495-m-thick Moià-Santpedor composite section, together with previous bio- and magnetostratigraphic studies in the Ebro Basin; confirms an earliest Oligocene age (~33.4 Ma) for the post- Grande Coupure Santpedor fossil site. This, in turn supports the close correlation between the dramatic terrestrial faunal turnover known as the Grande Coupure and the Eocene–Oligocene transition, with a (maximum) lag of time of 0.5 Myr. As in other Eocene–Oligocene records of Eurasia, in the Eastern Ebro Basin, the Grande Coupure might coincide with a shift to drier climatic conditions, as it has been deduced from sedimentological evidences, which includes incision of fluvial fan channel deposits as a consequence of the drop of the base level at a regional scale.

The precise Eocene–Oligocene continental chronology of the Ebro Basin allows an alternative interpretation of the Hampshire Basin sedimentary record (Isle of Wight, UK) which reconciles all the available marine and continental biostratigraphy from the Solent Group succession. From the integration of the Ebro and Hampshire basin records, a magnetostratigraphy-based calibration of the Late Eocene–Oligocene European mammal biochronology (MP reference levels) has resulted.

Supplementary materials related to this article can be found online at doi:10.1016/j.palaeo.2011.01.005.

Acknowledgements

This paper has been developed in the framework of the Spanish MCI projects: CENOCRON CGL2004-00780 and REMOSS 3D-4D CGL2007-66431-C02-02/BTE. This research was supported by the Research Group of "Geodinàmica i Anàlisi de Conques" (2009 GGR 1198 — Comissionat d'Universitats i Recerca de la Generalitat de Catalunya) and the Research Institute GEOMODELS. The authors wish to thank Bet Beamud from the "Laboratori de Paleomagnetisme" (Serveis Cientificotècnics UB-CSIC) and Dr. Cor Langereis from the Paleomagnetic Laboratory "Fort Hoofddijk" (Utrecht Universiteit). We are grateful to Mireia Butillé and Rubén Calvo who assisted during field work and the laboratory analysis. The comments and suggestions of Jaume Dinarès-Turell and Jerry Hooker have significantly improved this paper. E.C. was funded by a PhD grant of the Spanish MCI.

References

Aguilar, J.P., Legendre, S., Michaux, J., 1997. Actes du Congrès BiochroM'97. Mémoires et Travaux de l'Institut de Montpellier, Montpellier.

Agustí, J., Anadón, P., Arbiol, S., Cabrera, L., Colombo, F., Sáez, A., 1987. Biostratigraphical characteristics of the Oligocene sequences of North–Eastern Spain (Ebro and Campins Basins). Münchner Geowissenschaftliche Abhandlungen 10, 35–42.

Akhmetiev, M.A., Beniamovski, V.N., 2009. Paleogene floral assemblages around epicontinental seas and straits in Northern Central Eurasia: proxies for climatic and paleogeographic evolution. Geologica Acta 7 (1–2), 297–309. doi:10.1344/105.000000278.

Anadón, P., Vianey-Liaud, M., Cabrera, L., Hartenberger, J.L., 1987. Gisements à vertébrés du paléogène de la zone orientale du bassin de l'Ebre et leur apport à la stratigraphie. Paleontologia i Evolució 21, 117–131.

Anadón, P., Cabrera, L., Colldeforns, B., Colombo, F., Cuevas, J.L., Marzo, M., 1989. Alluvial fan evolution in the SE Ebro Basin: Response to tectonics and lacustrine base level changes. Excursion Guidebook. 4th International Conference on Fluvial Sedimentology. Publicacions del Servei Geològic de Catalunya, Barcelona.

Anadón, P., Cabrera, L., Choi, S.J., Colombo, F., Feist, M., Sáez, A., 1992. Biozonación del Paleógeno continental de la zona oriental de la Cuenca del Ebro mediante carófitas; implicaciones en la biozonación general de carófitas de Europa occidental. Acta Geologica Hispánica 27 (1–2), 69–94.

Arbiol, S., Sáez, A., 1988. Sobre la edad oligocénica inferior del yacimiento de Santpedor (Cuenca del Ebro, provincia de Barcelona). Acta Geologica Hispánica 23 (1), 47–50.

Arenas, C., Millán, H., Pardo, G., Pocoví, A., 2001. Ebro Basin continental sedimentation associated with late compressional Pyrenean tectonics (north–eastern Iberia): controls on basin margin fans and fluvial systems. Basin Research 13, 65–89.

Badiola, A., Checa, L., Cuesta, M.A., Quer, R., Hooker, J.J., Astibia, H., 2009. The role of new Iberian finds in understanding European Eocene mammalian paleobiogeography. Geologica Acta 7 (1–2), 243–258. doi:10.1344/105.000000281.

Barberà, X., 1999. Magnetostratigrafia de l'Oligocè del sector sud-oriental de la Conca de l'Ebre: implicacions magnetobiocronològiques i seqüencials. PhD thesis, Universitat de Barcelona, 247 pp.

Barberà, X., Cabrera, L., Marzo, M., Parés, J.M., Agustí, J., 2001. A complete terrestrial Oligocene magnetostratigraphy from the Ebro Basin, Spain. Earth and Planetary Science Letters 187 (1–2), 1–16. doi:10.1016/S0012-821(01)00270-9.

Berggren, W.A., Prothero, D.R., 1992. Eocene–Oligocene climatic and biotic evolution: an overview. In: Prothero, D.R., Berggren, W.A. (Eds.), Eocene–Oligocene climatic and biotic evolution. Princeton University Press, Princeton, pp. 1–28.

Cande, S.C., Kent, D.V., 1995. Revised calibration of the geomagnetic polarity time scale for the Late Cretaceous and Cenozoic. Journal of Geophysical Research 100, 6093–6095.

Cascella, A., Dinarès-Turell, J., 2009. Integrated calcareous nannofossil biostratigraphy and magnetostratigraphy from the uppermost marine Eocene deposits of the southeastern Pyrenean foreland basin: evidences for marine Priabonian deposition. Geologica Acta 7 (1–2), 281–296. doi:10.1344/105.000000282.

Cavagnetto, C., Anadón, P., 1996. Preliminary palynological data on floristic and climatic changes during the Middle Eocene-Early Oligocene of the eastern Ebro Basin, northeast Spain. Review of Palaeobotany and Palynology 92 (3–4), 281–305. doi:10.1016/0034-6667(95)00096-8.

Channell, J.E.T., Galeotti, S., Martin, E.E., Billups, K., Scher, H.D., Stoner, J.S., 2003. Eocene to Miocene magnetostratigraphy, biostratigraphy, and chemostratigraphy at ODP Site 1090 (sub-Antarctic South Atlantic). Geological Society of America Bulletin 11 (5), 607–623. doi:10.1130/0016-7606(2003.

Collinson, M.E., Hooker, J.J., 2003. Paleogene vegetation of Eurasia: framework for mammalian faunas. Deinsa 10, 41–84.

Coney, P.J., Muñoz, J.A., McClay, K.R., Evenchick, C.A., 1996. Syntectonic burial and post-tectonic exhumation of southern Pyrenees foreland fold-thrust belt. Journal of the Geological Society of London 153, 9–16.

Costa, E., Garcés, M., López-Blanco, M., Beamud, E., Gómez-Paccard, M., Larrasoaña, J.C., 2010. Closing and continentalization of the South Pyrenean foreland Basin (NE Spain): magnetochronological constraints. Basin Research 22, 904–917. doi:10.1111/j.1365-2117.2009.00452.x.

Cuevas, J.L., Cabrera, L., Marcuello, A., Arbués, P., Marzo, M., Bellmunt, F., 2010. Exhumated channel sandstone networks within fluvial fan deposits from the Oligo–Miocene Caspe Formation, South–east Ebro Basin (North–east Spain). Sedimentology 57, 162–189. doi:10.1111/j.1365-3091.2009.01096.x.

Dekkers, M.J., Linssen, J.H., 1989. Rockmagnetic properties of fine-grained natural low-temperature haematite with reference to remanence acquisition mechanisms in red beds. Geophysical Journal International 99, 1–18.

Dupont-Nivet, G., Krijgsman, W., Langereis, C.G., Abels, H.A., Dai, S., Fang, X., 2007. Tibetan plateau aridification linked to global cooling at the Eocene–Oligocene transition. Nature 445, 635–638. doi:10.1038/nature/05516.

Feist, M., Anadón, P., Cabrera, L., Choi, S.J., Colombo, F., Sáez, A., 1994. Upper Eocene–Lowermost Miocene charophyte succession in the Ebro Basin (Spain). Contribution to the charophyte biozonation in Western Europe. Newsletters on Stratigraphy 30 (1), 1–32.

Ferrer, J., 1971. El Paleoceno y Eoceno del borde suroriental de la Depresión del Ebro (Cataluña). Memories Suisses de Paleontologie 90, 1–70.

Gale, A.S., Huggett, J.M., Pälike, H., Laurie, E., Hailwood, E.A., Hardenbol, J., 2006. Correlation of Eocene–Oligocene marine and continental records: orbital, cyclicity, magnetostratigraphy and sequence stratigraphy of the Solent Group, Isle of Wight, UK. Journal of the Geological Society 163, 401–415. doi:10.1144/0016-764903-175.

Gale, A.S., Huggett, J.M., Laurie, E., 2007. Discussion on the Eocene–Oligocene boundary in the UK. *Journal*, Vol. 163, pp. 401–415. Journal of the Geological Society 164, 685–688. doi:10.1144/0016-76492006-098.

Garcés, M., Krijgsman, W., Agustí, J., 2001. Chronostratigraphic framework and evolution of the Fortuna basin (Eastern Betics) since the Late Miocene. Basin Research 13, 199–216. doi:10.1046/j.1365-2117.2001.00144.x.

Gradstein, F.M., Ogg, J.G., Smith, A., 2004. A geologic time scale 2004. Cambridge University Press, Cambridge.

Hartenberger, J.L., 1973. Les rongeurs de l'Eocène d'Europe. Leur évolution dans leur cadre biogéographique. Mémoires du Muséum National d'Historie Naturelle, Sciences de la Terre 24 (3), 49–70.

Hooker, J.J., 1987. Mammalian faunal events in the English Hampshire Basin (late Eocene–early Oligocene) and their application to European biostratigraphy. Münchener Geowissenschaftliche Abhandlungen 10, 109–116.

Hooker, J.J., 1992. British mammalian paleocommunities across the Eocene–Oligocene transition and their environmental implications. In: Prothero, D.R., Berggren, W.A. (Eds.), Eocene–Oligocene Climatic and Biotic Evolution. Princeton University Press, Princeton, pp. 494–515.

Hooker, J.J., 2010. The "Grande Coupure" in the Hampshire Basin, UK: taxonomy and stratigraphy of the mammals on either side of this major Paleogene faunal turnover. In: Whittaker, J.E., Hart, M.B. (Eds.), Micropalaeontology, Sedimentary Environments and Stratigraphy: A Tribute to Dennis Curry (1912–2001): The Micropalaeontological Society, Special Publications, pp. 147–215. doi:10.1144/TMS004.8.

Hooker, J.J., Collinson, M.E., Sille, N.P., 2004. Eocene–Oligocene mammalian faunal turnover in the Hampshire Basin, UK: calibration to the global time scale and the major cooling event. Journal of the Geological Society 161, 161–172. doi:10.1144/0016-764903-091.

Hooker, J.J., Collinson, M.E., Grimes, S.T., Sille, N.P., Mattey, D.P., 2007. Discussion on the Eocene–Oligocene boundary in the UK. Journal, Vol. 163, pp. 401–415. Journal of the Geological Society 164, 685–688. doi:10.1144/0016-76492006-098.

Hooker, J.J., Grimes, S.T., Mattey, D.P., Collinson, M.E., Sheldon, N.D., 2009. Refined correlation of the UK Late Eocene–Early Oligocene Solent Group and timing of its climate history. In: Koeberl, C., Montanari, A. (Eds.), The Late Eocene Earth-Hothouse, Icehouse and Impacts: The Geological Society of America, Special Paper, 452, pp. 179–195. doi:10.1130/2009.2452(12.

Janis, C.M., 1993. Tertiary mammal evolution in the context of changing climates, vegetation, and tectonic events. Annual Reviews of Ecology and Systematics 24, 467–500.

Joomun, S.C., Hooker, J.J., Collinson, M.E., 2008. Dental wear variation and implications for diet: An example from Eocene perissodactyls (Mammalia). Palaeogeography, Palaeoclimatology, Palaeoecology 263 (3–4), 92–106. doi:10.1016/j.palaeo.2008.03.001.

Katz, M.E., Miller, K.G., Wright, J.D., Wade, B.S., Browning, J.V., Cramer, B.S., Rosenthal, Y., 2008. Stepwise transition from the Eocene greenhouse to the Oligocene icehouse. Nature Geoscience 1 (5), 329–334. doi:10.1038/ngeo179.

Kirschvink, J.L., 1980. The least-squares line and plane and the analysis of paleomagnetic data. Geophysical Journal of the Royal Astronomical Society 62, 699–718.

Köhler, M., Moyà-Solà, S., 1999. A finding of Oligocene primates on the European continent. Proceedings of the National Academy of Sciences 96 (25), 14664–14667.

Lanci, L., Lowrie, W., Montanari, A., 1996. Magnetostratigraphy of the Eocene/Oligocene boundary in a short drill-core. Earth and Planetary Science Letters 143, 37–48.

Legendre, S., 1987. Les immigrations de la "Grande Coupure" sont-elles contemporaines en Europe occidentale? Münchner Geowissenschaftliche Abhandlungen 10, 141–148.

Legendre, S., Hartenberger, J.L., 1992. Evolution of mammalian faunas in Europe during the Eocene and Oligocene. In: Prothero, D.R., Berggren, W.A. (Eds.), Eocene–Oligocene Climatic and Biotic Evolution. Princeton University Press, Princeton, pp. 516–528.

Lowrie, W., 1990. Identification of ferromagnetic minerals in a rock by coercivity and unblocking temperature properties. Geophysical Research Letters 17 (2), 159–162.

Lowrie, W., Lanci, L., 1994. Magnetostratigraphy of the Eocene–Oligocene boundary sections in Italy: No evidence for short subchrons within chrons 12R and 13R. Earth and Planetary Science Letters 126, 247–258.

Luzón, A., González, A., Muñoz, A., Sánchez-Valverde, B., 2002. Upper Oligocene–Lower Miocene shallowing-upward lacustrine sequences controlled by periodic and non-periodic processes (Ebro Basin, northeastern Spain). Journal of Paleolimnology 28, 441–456. doi:10.1023/A:1021675227754.

Meng, J., McKenna, M.C., 1998. Faunal turnovers of Paleogene mammals from the Mongolian Plateau. Nature 394, 364–367. doi:10.1038/28603.

Muñoz, J.A., 1992. Evolution of a continental collision belt: ECORS-Pyrenees crust balanced cross-section. In: McClay, K.R. (Ed.), Thrust Tectonics. Chapman & Hall, London, pp. 235–246.

Ortí, F., Rosell, L., Inglès, M., Playa, E., 2007. Depositional models of lacustrine evaporites in the SE margin of the Ebro Basin (Paleogene, NE Spain). Geologica Acta 5 (1), 19–34.

Pallí, L., 1972. Estratigrafía del Paleógeno del Empordà y zonas limítrofes. PhD thesis, Universitat Autònoma de Barcelona, 338 pp.

Parés, J.M., Lanci, L., 2004. A Middle Eocene – Early Miocene Magnetic Polarity Stratigraphy in Equatorial Pacific Sediments (ODP Site 1220). In: Channell, J.E.T., Kent, D.V., Lowrie, W., Meert, J.G. (Eds.), Timescales of the Paleomagnetic Field: Geophysical Monograph Series, 145, pp. 131–140.

Prothero, D.R., 1994. The late Eocene–Oligocene extinctions. Annual Reviews of the Earth and Planetary Sciences 22, 145–165. doi:10.1146/annurev.ea.22.050194.001045.

Prothero, D.R., Swisher III, C.C., 1992. Magnetostratigraphy and geochronology of the terrestrial Eocene–Oligocene transition in North America. In: Prothero, D.R., Berggren, W.A. (Eds.), Eocene–Oligocene Climatic and Biotic Evolution. Princeton University Press, Princeton, pp. 46–73.

Puigdefàbregas, C., Souquet, P., 1986. Tecto-sedimentary cycles and depositional sequences of the Mesozoic and Tertiary from the Pyrenees. Tectonophysics 129, 173–203. doi:10.1016/0040-1951(86)90251-9.

Puigdefàbregas, C., Muñoz, J.A., Marzo, M., 1986. Thrust belt development in the eastern Pyrenees and related depositional sequences in the southern foreland basin. In: Allen, P.A., Homewood, P. (Eds.), Foreland Basins: Special Publication of the International Association of Sedimentologists, 8, pp. 229–246. Blackwell Scientific, Oxford.

Pujalte, V., Schmitz, B., Baceta, J.I., Orue-Etxebarria, X., Bernaola, G., Dinarès-Turell, J., Payros, A., Apellaniz, E., Caballero, F., 2009. Correlation of the Thanetian–Ilerdian turnover of larger foraminifera and the Paleocene–Eocene thermal maximum: confirming evidence from the Campo area (Pyrenees, Spain). Geologica Acta 7 (1–2), 161–175. doi:10.1344/105.000000276.

Riba, O., Reguant, S., Villena, J., 1983. Ensayo de síntesis estratigráfica y evolutiva de la cuenca terciaria del Ebro. In: Comba, J.A. (Ed.), Geología de España. Libro Jubilar J.M. Ríos, Tomo II. Publicaciones del Instituto Geológico y Minero de España (IGME), Madrid, pp. 131–159.

Sáez, A., 1987. Estratigrafía y sedimentología de las formaciones lacustres del tránsito Eoceno–Oligoceno del noreste de la cuenca del Ebro. PhD thesis, Universitat de Barcelona, 353 pp.

Sáez, A., Anadón, P., Herrero, M.J., Moscariello, A., 2007. Variable style of transition between Palaeogene fluvial fan and lacustrine systems, southern Pyrenean foreland, NE Spain. Sedimentology 54, 367–390. doi:10.1111/j.1365-3091.2006.00840.x.

Schmidt-Kittler, N., 1987. European reference levels and correlation tables. Münchener Geowissenschaftliche Abhandlungen 10, 13–32.

Serra-Kiel, J., Travé, A., Mató, E., Saula, E., Ferràndez-Cañadell, C., Busquets, P., Tosquella, J., Vergés, J., 2003. Marine and transitional Middle/Upper Eocene Units of the Southeastern Pyrenean Foreland Basin (NE Spain). Geologica Acta 1 (2), 177–200.

Stehlin, H.G., 1910. Remarques sur les faunules de Mammifères des couches Éocènes et Oligocènes du Bassin de Paris. Bulletin de la Societe Geologique de France 9 (4), 488–520.

Tobien, H., 1987. The Position of the "Grande Coupure" in the Paleogene of the Upper Rhine Graben and the Mainz Basin. Münchner Geowissenschaftliche Abhandlungen 10, 197–202.

Vergés, J., Marzo, M., Santaeulària, T., Serra-Kiel, J., Burbank, D.W., Muñoz, J.A., Giménez-Montserrat, J., 1998. Quantified vertical motions and tectonic evolution of the SE Pyrenean foreland basin. In: Mascle, A., Puigdefàbregas, C., Luterbacher, H.P., Fernàndez, M. (Eds.), Cenozoic Foreland Basins of Western Europe: Geological Society Special Publication, 134, pp. 107–134.

Vergés, J., Fernàndez, M., Martínez, A., 2002. The Pyrenean orogen: pre-, syn-, and post-collisional evolution. In: Rousenbaum, G., Lister, L.G. (Eds.), Reconstruction of the Evolution of the Alpine-Himalayan Orogen: Journal of the Virtual Explorer, 8, pp. 55–74. doi:10.3809/jvirtex.2002.00058.